Journal of Thermal Analysis and Calorimetry
https://doi.org/10.1007/s10973-020-09349-9

CO_2 mineralization by burnt oil shale and cement bypass dust: effect of operating temperature and pre-treatment

Can Rüstü Yörük[1] · Mai Uibu[1] · Mustafa Cem Usta[1] · Tiit Kaljuvee[1] · Andres Trikkel[1]

Received: 31 July 2019 / Accepted: 13 January 2020
© Akadémiai Kiadó, Budapest, Hungary 2020

Abstract
The alkaline wastes such as burnt oil shale (BOS) and cement bypass dust (BPD) generally contain free lime and portlandite which make them suitable sorbent materials for CO_2 trapping via mineral carbonation technique of carbon capture and sequestration. In order to study the reaction kinetics and effect of operating parameters on carbonation processes of such alkaline wastes for future industrial sized scale-ups, as well as to identify the effects on carbonation capacity when these sorbents undergo pre-treatment and are exposed to different temperatures, BOS and BPD as sorbents in CO_2 mineralization process have been investigated with thermal analysis methods in the current work. Results indicate that selected types of BOS and BPD could be used as binders in the CO_2 mineralization systems, binding reasonably good amount of CO_2 already in the early stage of the carbonation process which later slows down as the rate of CaO carbonation becomes mainly diffusion controlled. Increased process temperature and hydration as pre-treatment improve the CO_2 binding ability, while the effect of milling has been found to be staggering and not as significant as the effect of hydration and temperature rise. The appropriate kinetic mechanism functions were determined, and the kinetic parameters—activation energy (E_a) and pre-exponential factor (A) values were calculated for all the samples. The E_a values of hydrated samples are lower for BOS samples compared to non-hydrated samples. It was shown that activation by hydration enables to reach the same CO_2 uptake levels at lower temperatures, thereby making the mineralization process more energy efficient and thus lowering the costs.

Keywords CCS · Mineral carbonation · Oil shale ash · Bypass dust

Introduction

The exploitation of fossil fuels for industrial and home uses results in atmospheric emissions of CO_2 and the production of other greenhouse gases that have deleterious effects on the planet's environment. Environmentally unsafe disposal of ashes which are produced from fossil fuel combustion is also additional negative side effect of fossil fuel combustion. Many approaches have been developed to reduce CO_2 emissions, and carbon capture and sequestration (CCS) has been the limelight as the most promising method [1–3].

Mineral carbonation is one of the alternative CCS applications that can contribute to reduction in CO_2 emissions and provide another advantageous way to geological storage and help the world's transition to a lower-carbon economy. Mineral carbonation is a relatively new idea emerging in the early 90s in CCS technologies that aimed to mitigate CO_2 emissions. Seifritz first described it in 1990 as a binding method for CO_2 [4]. This was further explained by Dusmore in 1992 who added studies related to CO_2 binding possibilities of calcium- and magnesium-bearing minerals [5]. Lackner et al. further expanded these studies in 1995 establishing silicate minerals (olivine, serpentine and wollastonite) and also basalt rock as the most suitable natural raw materials that are both cheap and abundant in the world. His contributions paved the way for an acceleration of the research in this field and established mineral carbonation as a viable technique that is still utilized in the present day research [6]. Mineral carbonation otherwise called "mineral sequestration" includes a procedure where CO_2 from a capture step is carried into contact with a metal oxide-bearing materials and silicates that contains alkaline earth metals (e.g., calcium and magnesium), with the aim of fixing the CO_2 as insoluble carbonates [7].

✉ Can Rüstü Yörük
can.yoruk@taltech.ee

[1] Department of Materials and Environmental Technology, Tallinn University of Technology, Ehitajate tee 5, 19086 Tallinn, Estonia

Published online: 29 January 2020

The most suitable feedstocks for mineral CO_2 sequestration from natural minerals are the alkaline earth metals containing calcium and magnesium which are widely available. Another option for feedstocks is calcium-rich alkaline solid wastes from industry that can be used in particular applications for CO_2 sequestration. As an alternative to natural minerals, idea of using industrial wastes as a feedstock for CO_2 mineralization has been researched [8–12]. Since the industrial residues tend to be chemically more unstable and more active compared to natural minerals, the energy intensity of the process could be lower. Direct carbonation methods involving gas–solid or gas–liquid–solid processes are more attractive for industrial wastes because of the diversity of elements that are present in wastes which would affect the recovery of solvent. Also, the environmental considerations suggest that the product of direct carbonation process would be better for environment because the solid matrix that can retain contaminants is not demolished in the process and thus does not contribute to the leaching of heavy metals [8–12].

Major industrial wastes include ashes from combustion processes as the fossil fuel-power industry produces a lot of ash during the coal and oil shale (OS) conversion in thermal power plants producing mainly bottom and fly ashes. These ashes have often a mixed and varied composition resulting from differences in the type and rank of coal and OS (or the type and process of fuel treatment) where free CaO content (mass basis) ranges between 1% in bituminous coal ashes and up to 30% in BOS [8, 9]. Incinerator sewage sludge ash also emerges from combustion of sludge leftover and produces a silty-sandy textured sludge ash rich in CaO and MgO content (30% and 3%, respectively) [10]. The residues of biomass and wood ash also act as good raw materials for direct carbonation and sequestration. These residues are produced through combustion and usually contain powdery granulated amorphous particles, where the free CaO content varies in relation to the nature of biomass and wood burned and ranges from 24 to 46% [11].

Different types of ashes and wastes are also abundantly produced in the cement industry including cement kiln dust (CKD), cement bypass dust (CBPD), ordinary portland cement, recycled concrete aggregate (RCA), etc. Although RCA is the main waste stream of this category, CKD and CBPD which are fine by-products of portland cement also have great carbonation potential because of their favorable free lime content due to the high-temperature rotary kiln production operations. CKDs are captured in the air pollution control dust collection system. Ca content in this waste stream can usually be as high as 35.5% [12]; however, since it does not have high content of free CaO, it is not suitable for carbonation. CBPD on the other hand is rich in Ca which is found as free CaO and portlandite, so, it is a suitable candidate for mineral carbonation.

Metal waste streams are also considered to have potential as CO_2 sorbents. Some of these metal industry wastes are air- or water-cooled copper slag, phosphorus slag, ground-granulated blast furnace slag and steel slag. Besides, there are alternative minor waste products including red sludge, air pollution control residues and paper sludge which also have appropriate chemical composition for mineral carbonation [13–19].

Mineral carbonation by industrial waste is a prominent option of CCS for countries with no geological storage option, such as Estonia. The question of utilization of solid wastes and long-term sustainability in OS and cement sectors still remains as a key issue due to the huge amounts of waste produced every year. By means of adopting new technologies with low carbon emissions to cope with similar environmental concerns, CO_2 capture using alternative solid adsorbents attracts a great attention due to future emission targets of the countries.

Although mineral carbonation studies of different waste materials with different process routes have been conducted around the world [20–26], there are a limited number of papers specifically related to direct gas–solid carbonation of BOS and CBPD. In order to overcome slow carbonation of these industrial wastes with the technology that can be operated at a wide range of temperatures; from ambient to typical calcium looping (CaL) ones, some pre-treatment can be required or process temperatures are needed to be optimized due to the energy intensity of the applications and the effects of pre-treatment and temperature on CO_2 capture capacities and capabilities have to be investigated to obtain preliminary knowledge for future industrial applications of mineral carbonation.

This study focuses on direct mineral carbonation of two different BOS and CBPD residues under atmospheric pressure conditions with 100% CO_2 in order to obtain both experimental and operational knowledge by studying thermal characteristics of CO_2 mineralization, clarifying reaction mechanisms and kinetics and investigating the effect of pre-treatment (hydration and grinding) at different process temperatures. The main objectives are to make pre-evaluation of carbonation potentials of the selected samples, compare the CO_2 uptake capacities and evaluate the effect of activation by hydration and grinding on reactivity as well as to investigate the applicability of the carbonation process in larger scale by using rotating tube furnace.

Materials and methods

Sample preparation

Three different types of waste residues from OS and cement industry were chosen and named as BOS1 which represents

burnt OS samples from total ash silo of circulating fluidized bed (CFB) boilers of Balti power plant in Estonia, BOS2 which represents burnt OS samples from the electrostatic precipitators of Auvere power plant also located in Estonia and BPD representing the cement bypass dust obtained from Robilante (Italy) cement factory (as an example of the local cement industry). The samples for each residue have been prepared as hydrated, non-hydrated and ground.

The hydrated samples have been prepared with liquid to solid ratio of 0.2 w/w in a semi-batch Eirich EL1 type intensive mixer. The samples were mixed with water at a rotation speed of 300 rpm for 20 min. Later, hydrated samples were dried at 105 °C for 4 h (other samples as well before isothermal tests). As an additional pre-treatment, each sort of samples has also been ground in a Retsch PM 100 grinding machine (5 min) in a four-ball planetary mill.

Experimental

The Setaram Labsys 2000 thermoanalyzer was used to investigate the mass gain representing the CO_2 uptake during the carbonation of BOS1, BOS2 and BPD. During the experiments, standard 100 µL Al_2O_3 crucibles were used and mass of the samples was 10 ± 0.5 mg. The isothermal tests were performed at four different temperatures (300, 400, 450 and 500 °C) for hydrated samples and for original (non-hydrated) samples at seven different temperatures (300, 400, 450, 475, 500, 550 and 600 °C) for 30 min. Hydrated samples were not tested at 550 and 600 °C in order to eliminate the dihydroxylation of the $Ca(OH)_2$ particles which can occur in the temperature range of 500 and 600 °C. Ground samples were also tested at 400, 500 and 600 °C. Overall temperatures higher than 600 °C were excluded in order to test the applicability of more energy efficient process at somewhat lower temperatures compared to well-known CaL process with the carbonation temperature of 650–700 °C. All thermogravimetric (TG) tests were carried out in 100% CO_2 atmosphere by switching the inert atmosphere of 100% Ar to CO_2 when desired temperature is reached. The flow of CO_2 was kept constant at 50 mL min^{-1} across all experiments.

Additionally, Nabertherm rotating tube furnace with parameters, T max of 1200 °C, furnace tube diameter of 70–90 mm, was operated for bigger scale gas solid carbonation of the samples in order to determine the applicability of the process to wider scale operations. 200 g hydrated and non-hydrated samples was led into the horizontal quartz tube furnace. The samples were heated in the atmosphere of 100% N_2 up to 400 ± 10 °C, and then, CO_2 gas was fed into the tube furnace for 30 min. Rotation speed was kept at 5 rpm in order to enable easier solid–gas contact and diffusion of CO_2. CO_2 entered the tube at the inlet with a rate of 100 L h^{-1} during the isothermal process. After cooling, analytical samples were taken for determination of the mineral CO_2 and free CaO content. The initial and carbonated samples were analyzed also with FTIR spectrometer ALPHA in order to compare mineralogical changes. FTIR measurements were recorded in the 400–4000 cm^{-1} region.

Characterization of samples

The materials were analyzed also using XRF spectroscopy (Rigaku Primus II) and quantitative X-ray diffraction (XRD, Bruker D8 Advanced). The contents of free lime (fCaO), by ethylene glycol method (Reispere 1966) and mineral CO_2 using Electra CS-580 Carbon/Sulfur Determinator were determined. In addition, the Brunauer–Emmett–Teller (BET) SSA and the particle size distribution (PSD) were determined using a Kelvin 1042 sorptometer and Horiba laser scattering particle size distribution analyzer LA-950, respectively.

It is known that the carbonation of lime is shown to be very much dependent on the SSA of the hydrated lime particles [27]. It is also known that hydration of lime increases SSA of the particles [28]. From BET SSA tests, it can be seen that the SSA of all the samples has increased after initial hydration (see Fig. 1). The highest increase has occurred on BPD, the initial sample had SSA of 3.84 m^2 g^{-1} with mean particle size of 40.87 µm; after hydration, it rose to 7.02 m^2 g^{-1}. The highest SSA belonged to BOS2 before hydration with a mean particle size of 20.98 µm and SSA

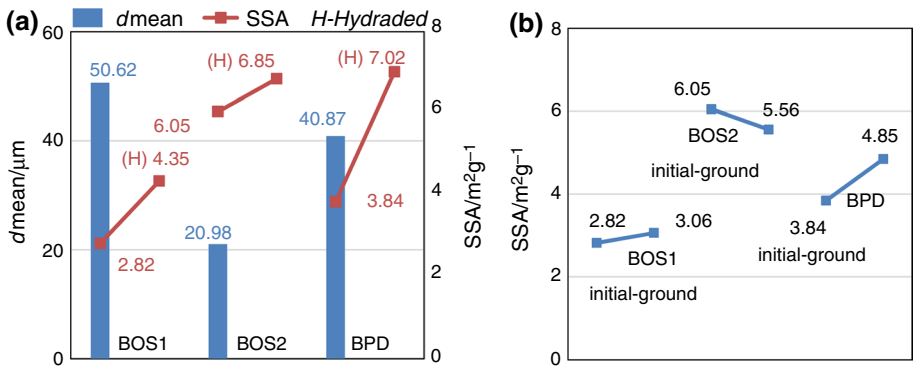

Fig. 1 Mean particle size and BET SSA of the samples after hydration (**a**) and BET SSA of the samples after grinding (**b**)

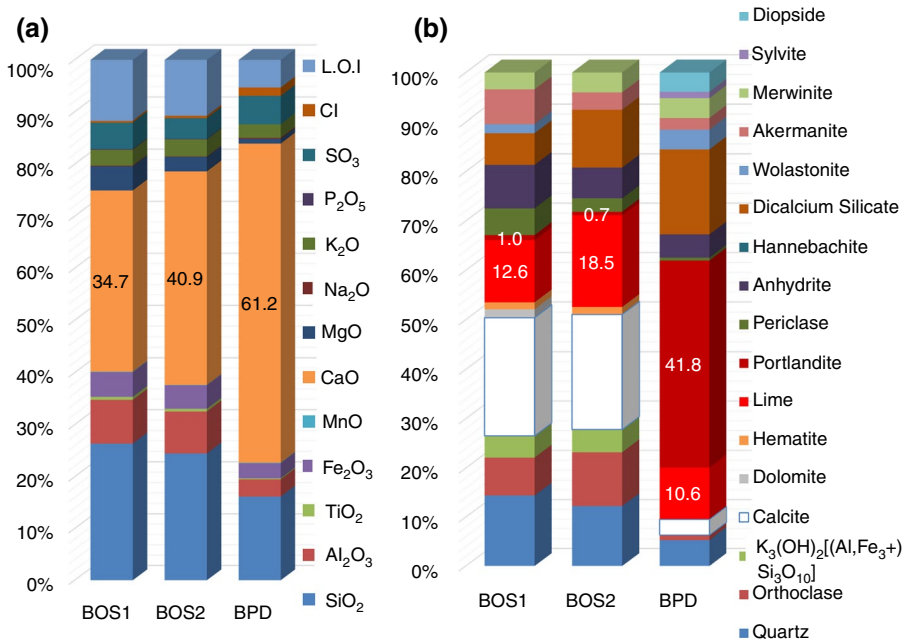

Fig. 2 Chemical composition of the samples (**a**) and phase composition of the samples (**b**)

of 6.05 $m^2\ g^{-1}$, increasing to 6.85 $m^2 g^{-1}$ after hydration. BOS1 with a mean particle size of 50.62 µm had SSA of 2.82 $m^2 g^{-1}$ which increased to 4.35 $m^2\ g^{-1}$ after hydration. Grinding has increased the SSA of BOS1 and BPD while decreasing SSA of BOS2 (see Fig. 1b).

pre-inspection of the hydrated samples, the measured mass loss due to dehydration indicates the increase (~3%) in the hydrated compound (free CaO, C2S, etc.) forming $Ca(OH)_2$.

In order to estimate and compare the CO_2 binding ability of different samples, CO_{2max}, maximal possible CO_2 uptake capacity of the samples was calculated on the basis of $Ca(OH)_2$ (taking into account its CaO as free CaO), free CaO, $CaSiO_3$, Ca_2SiO_4 and $Ca_3Mg(SiO_4)_2$ content of initial sample as shown below (Eq. 1).

$$CO_{2max} = \frac{\frac{fCaO \times M_{CO_2}}{M_{CaO}} + \frac{CaSiO_3 \times M_{CO_2}}{M_{CaSiO_3}} + \frac{2 \times Ca_2SiO_4 \times M_{CO_2}}{M_{Ca_2SiO_4}} + \frac{3 \times Ca_3Mg(SiO_4)_2 \times M_{CO_2}}{M_{Ca_3Mg(SiO_4)_2}} + CO_2}{100 + \frac{fCaO \times M_{CO_2}}{M_{CaO}} + \frac{CaSiO_3 \times M_{CO_2}}{M_{CaSiO_3}} + \frac{2 \times Ca_2SiO_4 \times M_{CO_2}}{M_{Ca_2SiO_4}} + \frac{3 \times Ca_3Mg(SiO_4)_2 \times M_{CO_2}}{M_{Ca_3Mg(SiO_4)_2}}} \times 100\%. \quad (1)$$

Chemical and phase composition

According to XRF analysis, the BOS samples and the BPD compose of mainly Ca and Si compounds adding up 60–75%. The sample of BPD contains considerable amount of free lime and portlandite; total CaO content is 61.2% (see Fig. 2a). Additionally, it contains 17.2% dicalcium silicate, 4.0% wollastonite and 4.0% merwinite that could also be considered as CO_2 binding minerals (see Fig. 2b). The content of quartz, calcite and anhydrite is 5.3%, 3.2% and 4.7%, respectively. The quantitative XRD analysis indicated that samples contained considerable amount of lime, portlandite and secondary Ca–silicates, which attribute as potential CO_2 binders (see Fig. 2b) as the BOS samples also have reasonably high amounts of free lime (BOS1-12.6% and BOS2-18.5%). Additionally, based on the TG tests performed for

Results and discussion

Isothermal tests

Thermal analysis of BOS1, BOS2 and BPD is presented in Figs. 3–5 representing the CO_2 uptake ($mgCO_2$/10 mg sample) curves in 100% CO_2 atmosphere. The curves that were obtained at lower temperatures have not been added as they have shown negligible carbonation rates for the non-hydrated samples.

The non-hydrated BOS1 sample has quite similar final CO_2 uptake values also at 400–500 °C, while hydrated BOS1 sample has substantial difference in CO_2 uptake values at the same temperatures being much higher (see Fig. 3). Increased temperatures show increasing CO_2 uptake capacities for BOS1 and all other samples as well.

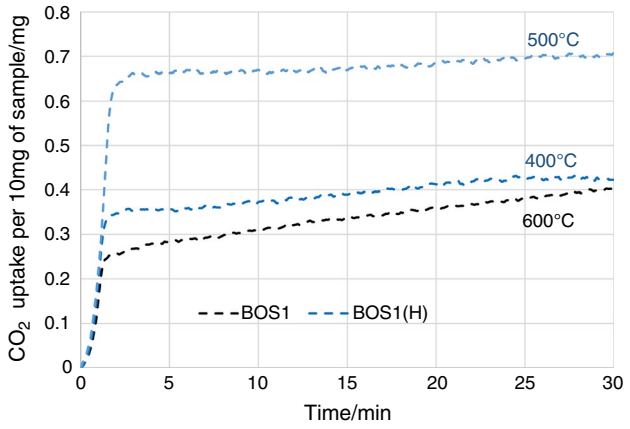

Fig. 3 BOS1 isothermal TG curves (H-hydrated)

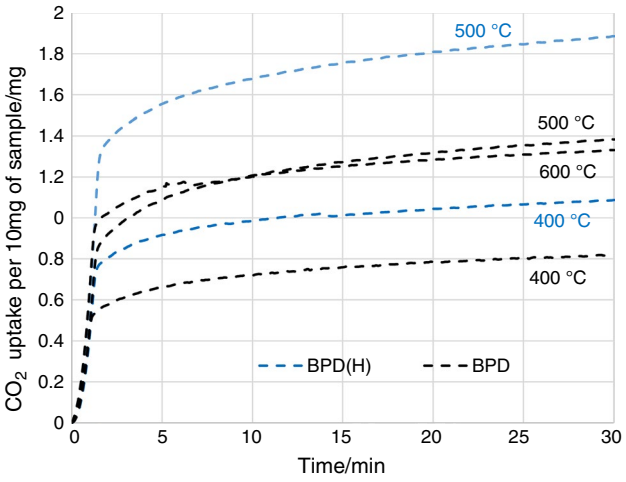

Fig. 5 BPD isothermal TG curves (H-hydrated)

Changes in CO_2 uptake levels with increasing temperatures are more clearly expressed for the hydrated samples (see Fig. 4) (0.58 → 0.85 mg CO_2/10 mg BOS2(H), 1.1 → 1.9 mg CO_2/10 mg BPD(H) at 400–500 °C) in comparison to non-hydrated samples (0.43 → 0.55 mg CO_2/10 mg BOS2, 0.9 → 1.4 mg CO_2/10 mg BPD at 400–500 °C). This proves that activation by hydrating (liquid to solid ratio of 0.2 w/w) of industrial residues can increase CO_2 uptake potential in all samples. Approximately, 80% of the CO_{2max} can been reached in all hydrated samples in first 2–3 min at 500 °C, and later on, the carbonation process gradually slows down and free CaO content is nearly exhausted after 30 min of treatment for hydrated samples. TG tests indicate that the carbonation process is quite fast at the first stage due to the large reaction surface available, and after 2 min, it slows down due to the decrease in surface area and increasing product layer diffusion resistance [29].

Curves of non-hydrated BPD sample show that at 500 and 600 °C CO_2 uptake values are quite similar which can be interpreted so that temperature increase does not increase the CO_2 uptake values at this interval anymore (see Fig. 5), and possible dehydration reaction with mass loss can also start at this temperature as it gets closer to the equilibrium temperature 500–550 °C (Eq. 2).

$$Ca(OH)_2 \rightarrow CaO + H_2O. \quad (2)$$

However, CO_2 uptake values of non-hydrated BOS1 and BOS2 samples increase at 600 °C compared to 500 °C. Results have shown that hydrated samples have gained the ability to bind more CO_2 for all the samples both at 400 and 500 °C. The non-activated samples have an initial binding rate comparable to the hydrated samples, yet the binding reaction tends to slow down at lower conversion levels which results in lower final CO_2 uptake values as compared to hydrated samples.

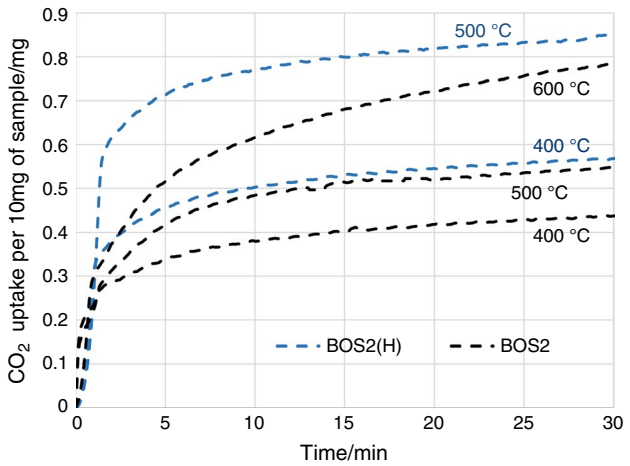

Fig. 4 BOS2 isothermal TG curves (H-hydrated)

Effect of mechanical treatment

As an additional pre-treatment method, the samples were ground in a Retsch PM 100 grinding machine (5 min) in a four-ball planetary mill. Although the BET surface area of BOS1 was increased from 2.83 to 3.06 $m^2\ g^{-1}$, and similarly, BPD BET surface area was also increased 3.84–4.85 $m^2\ g^{-1}$ after grinding (see Fig. 1), the ground samples that were tested at 400–500–600 °C showed an unexpected slight decrease in the reaction rates as well as in their binding capacity. For this reason, the TA curves for the ground samples have not been reproduced here.

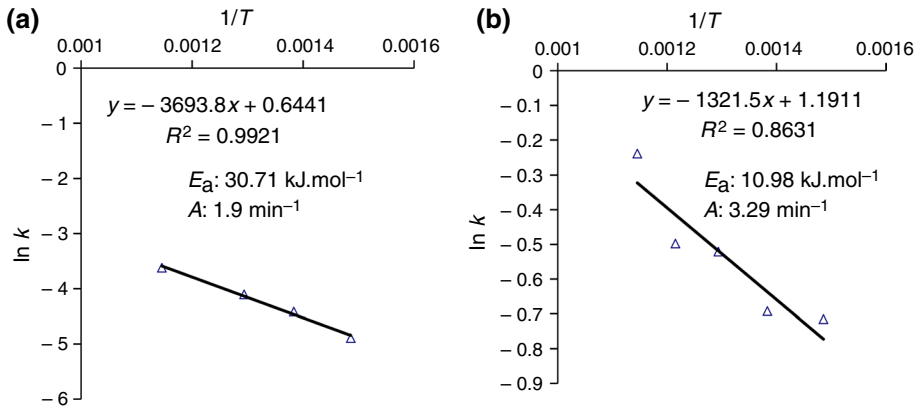

Fig. 6 Arrhenius plots of BOS2 (**a**) and BPD (**b**)

Kinetics

Calculations for the purpose of determining the reaction mechanism of the first fast stage of the carbonation reaction up to 2 min without including the second slow stage have been made based on the isothermal data and using different well-known reaction mechanisms [30]. The experimental data from isothermal tests at different temperatures were fitted to a set of kinetic models to give the highest regression.

The general equation for solid-state reaction kinetics is shown in Eq. (3):

$$f(\alpha) = (\mathrm{d}\alpha/\mathrm{d}t)/k \tag{3}$$

where $f(\alpha)$ is a certain mechanism function, t represents time, α is the extent of the reaction or fraction converted, and k is the rate constant. By integration of Eq. (4), we get:

$$g(\alpha) = \int \mathrm{d}\alpha/f(\alpha) = kt \tag{4}$$

where $g(\alpha)$ is the integral form of the kinetic model, the graph of $g(\alpha)$ versus the reaction time is a straight line, whose slope is the rate constant, k. Following this, the activation energy can be subsequently calculated from Arrhenius equation according to the graph of the logarithm of the rate constants versus the inverted temperature values (Eq. 5):

$$\ln(k) = \ln A - \frac{E_a}{RT}. \tag{5}$$

Table 1 k values for each temperature and linear correlation coefficient (R^2) for the most reasonable mechanism function, obtained E_a and A values for all samples

Sample →	BOS1	BOS1(H)	BOS2	BOS2(H)	BPD	BPD(H)
Model →	D3	A2	D3	A2	A2	A2
T/K	k/R^2	k/R^2	k/R^2	k/R^2	k/R^2	k/R^2
573	–	–	–	–	–	0.26
						0.822
673	0.0028	0.49	0.0075	0.47	0.49	0.54
	0.9563	0.942	0.8288	0.8397	0.8324	0.9497
723	0.0032	0.51	0.012	0.5	0.5	0.74
	0.9783	0.9641	0.9005	0.9769	0.9837	0.965
748	–	0.54	–	0.55	–	0.79
		0.9545		0.9745		0.9828
773	0.0046	0.63	0.017	0.68	0.59	0.97
	0.9576	0.9765	0.9801	0.9677	0.9604	0.9416
823	0.0065	–	–	–	0.61	–
	0.7898				0.9572	
873	0.029	–	0.028	–	0.78	–
	0.7976		0.9294		0.9417	
E_a/k J mol^{-1}	47.67	9.2	30.71	13.93	10.98	23.25
A/min^{-1}	12.47	2.5	1.9	5.5	3.29	34.94
R^2	0.8168	0.7321	0.9921	0.7921	0.8613	0.9963

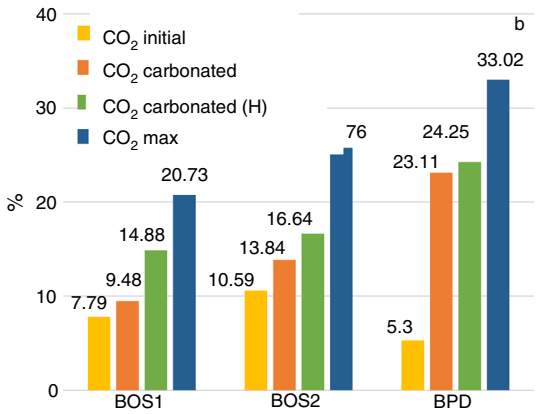

Fig. 7 Changes in mineral CO_2 content based on TIC measurements and CO_2 max according to Eq. 1

Based on the well-known reaction mechanisms [30] and the calculated regression coefficients, the most probable model for the carbonation process of non-hydrated BOS1 and BOS2 agrees with the three-dimensional diffusion model, D3 mechanism (Eq. 5), and the rate of CaO carbonation is mainly diffusion controlled.

$$D3:[1-(1-\alpha)^{1/3}]^2 = kt. \tag{6}$$

However, the most probable model for the carbonation process of all hydrated samples and non-hydrated BPD agrees with A2 model (Eq. 7) which is explained as random successive nucleation and nuclei growth model.

$$A2:[-\ln(1-\alpha)]^{0.5} = kt. \tag{7}$$

According to the selected most appropriate mechanism functions (D3, A2), the kinetic parameters have been calculated and the relationship between $1/T$ and $\ln k$ for BOS2 and BPD is shown in Fig. 6. According to the slopes and intercepts of the fitting straight lines, activation energy (E_a) and pre-exponential factor (A) values were obtained for all samples and are shown in Table 1.

At all selected temperatures, higher carbonation rates belong to the hydrated samples compared to non-hydrated samples. Although the rates are temperature sensitive, temperature rise is not as effective as hydration treatment even when the lowest and highest temperatures are compared in terms of the determined reaction rates. The hydration treatment is clearly more effective for BOS samples, especially, for BOS1; increasing the rates of carbonation reactions significantly at certain temperatures compared to non-hydrated cases. Due to the higher carbonation rates of hydrated BOS samples, the obtained E_a values are lower for hydrated samples, yet the hydration causes to increase in E_a value for the hydrated BPD.

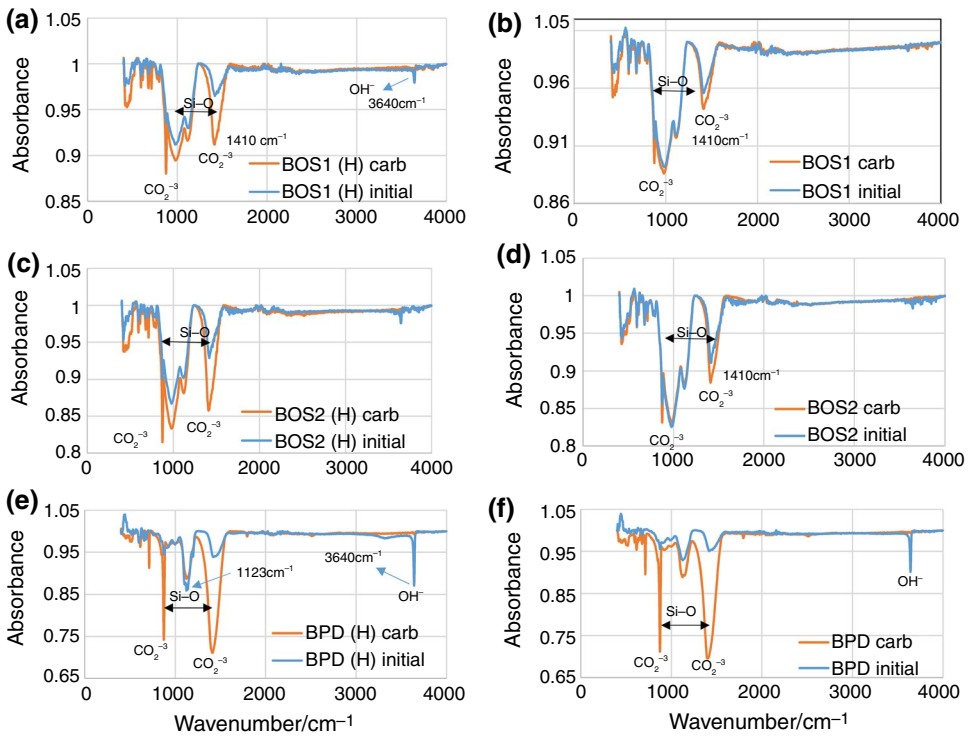

Fig. 8 FT-IR analysis BOS1[H-hydrated] (**a**), BOS1 (**b**), BOS2[H-hydrated] (**c**), BOS2 (**d**), BPD[H-hydrated] (**e**) and BPD (**f**)

Rotating tube furnace tests

Nabertherm rotating tube furnace was operated to re-evaluate the TG results with bigger amounts of samples and for bigger scale carbonation process tests. Overall, the measured mineral CO_2 levels (see Fig. 7) for all the samples after carbonation treatment in the rotating tube furnace were higher than the initial levels which shows that the carbonation tests with rotating tube furnace were successful. Due to rotation of the tube which increases gas–solid contact affecting positively the CO_2 diffusion in sample layer, the CO_2 uptake levels are higher—up to 0.15 kg CO_2 per kg of waste for BOS and 0.24 kg CO_2 per kg of waste for BPD compared to the results obtained from TG tests (0.045–0.082 kg CO_2 per kg of waste for BOS2 and BPD, respectively).

According to the FTIR analysis of the samples carbonated in the rotating tube furnace, the intensity of portlandite peaks (3640 cm^{-1}) decreases and of carbonates (872, 1417 cm^{-1}) increases after carbonation process (see Fig. 8a–f). Ca-bearing silicates (1123 cm^{-1}) play also a role in carbonation reactions of BPD as their intensities also slightly decrease (see Fig. 8e). For hydrated BOS samples also, the intensity of $Ca(OH)_2$ (3640 cm^{-1}) decreases after carbonation, while Ca–silicates (980, 1120 cm^{-1}) were not involved in carbonation process (see Fig. 8a–d). Peaks of the BOS1 and BOS2 spectra (1410–1415 cm^{-1}) clearly show that after hydration the binding reactivity and CO_2 uptake levels of BOS samples have been increased (see Fig. 8a,c).

Conclusions

In this paper, direct gas–solid mineral carbonation process with different industrial alkaline wastes including BOS and BPD was studied under isothermal heating conditions by using TG and tests in rotating tube furnace. The comparison of CO_2 uptake levels and reactivity during carbonation reactions of hydrated and non-hydrated samples has been given and explained in the context of this research. Based on the obtained experimental findings and kinetic calculations, the most probable model for the carbonation process of non-hydrated BOS1 and BOS2 agrees with the three-dimensional diffusion model (D3) and the most probable model for the carbonation process of the hydrated samples and non-hydrated BPD agrees with the random nucleation and nuclei growth model (A2). The notable positive effect of hydration treatment is that the same CO_2 uptake levels can be achieved at lower operating temperatures to minimize the heat requirements for preheating the solids, thereby making the carbonation processes of similar types of industrial wastes (which are widely available) more energy efficient and thus lowering the operational and energy costs.

Acknowledgements This project has received funding from the European Union's Horizon 2020 Framework Programme under Grant Agreement No. 764816 (CLEANKER) and from Institutional Research Funding of the Estonian Ministry of Education and Research, Grant No. IUT33-19.

References

1. Raza A, Gholami R, Rezaee R, Rasouli V, Rabiei M. Significant aspects of carbon capture and storage—a review. Petroleum. 2018. https://doi.org/10.1016/j.petlm.2018.12.007 **(in press)**.
2. Leung DYC, Caramanna G, Maroto-Valer MM. An overview of current status of carbon dioxide capture and storage technologies. Renew Sustain Energy Rev. 2014;39:426–43.
3. Bui M, et al. Carbon capture and storage (CCS): the way forward. Energy Environ Sci. 2018;11:1062–176.
4. Seifritz W. CO_2 disposal by means of silicates. Nature. 1990;345(6275):486–486.
5. Dunsmore H. A geological perspective on global warming and the possibility of carbon dioxide removal as calcium carbonate mineral. Energy Convers Manag. 1992;33(5–8):565–72.
6. Lackner KS, Wendt CH, Butt DP, Joyce EL, Sharp DH. Carbon dioxide disposal in carbonate minerals. Fuel Energy Abstr. 1995;36(6):457.
7. Metz B, Davidson O, Coninck H, Loos M, Meyer L. IPCC special report on carbon dioxide capture and storage. Cambridge: Cambridge University Press; 2005. p. 431.
8. Mazzella A, Errico M, Spiga D. CO_2 uptake capacity of coal fly ash: influence of pressure and temperature on direct gas-solid carbonation. J Environ Chem Eng. 2016;4(4):4120–8.
9. Sanna A, Uibu M, Caramanna G, Kuusik R, Maroto-Valer MM. A review of mineral carbonation technologies to sequester CO_2. Chem Soc Rev. 2014;43:8049–80.
10. Garcés P, Pérez Carrión M, García-Alcocel E, Payá J, Monzó J, Borrachero MV. Mechanical and physical properties of cement blended with sewage sludge ash. Waste Manag. 2008;28:2495–502.
11. Voshell S, Mäkelä M, Dahl O. A review of biomass ash properties towards treatment and recycling. Renew Sustain Energy Rev. 2018;96:479–86.
12. Abdel-Ghani NT, El-Sayed HA, El-Habak AA. Utilization of by-pass cement kiln dust and air-cooled blast-furnace steel slag in the production of some "green" cement products. HBRC J. 2018;14(3):408–14.
13. Gorai B, Jana RK, Premchand A. Characteristics and utilisation of copper slag—a review. Resour Conserv Recycl. 2003;39(4):299–313.
14. Shi C, Meyer C, Behnood A. Utilization of copper slag in cement and concrete. Resour Conserv Recycl. 2008;52(10):1115–20.
15. Li J, Lü Q, Liu X, Zhang S, Liu D. Phosphorus capacity of $CaO–SiO_2–Al_2O_3–MgO–Fe_xO$ slag. J Iron Steel Res Int. 2015;22(5):377–81.
16. Saluja S, Kaur K, Goyal S, Bhattacharjee B. Assessing the effect of GGBS content and aggregate characteristics on drying shrinkage of roller compacted concrete. Constr Build Mater. 2019;201:72–80.
17. Guo Y, Xie J, Zhao J, Zuo K. Utilization of unprocessed steel slag as fine aggregate in normal- and high-strength concrete. Constr Build Mater. 2019;204:41–9.

18. Ayres RU, Holmberg J, Andersson B. Materials and the global environment: waste mining in the 21st century. MRS Bull. 2001;26:477. https://doi.org/10.1557/mrs2001.119.
19. Sahu RC, Patel RK, Ray BC. Neutralization of red mud using CO_2 sequestration cycle. J Hazard Mater. 2010;179(1–3):28–34.
20. Bobicki ER, Liu Q, Xu Z, Zeng H. Carbon capture and storage using alkaline industrial wastes. Prog Energy Combust Sci. 2012;38(2):302–20.
21. Bertos MF, Li X, Simons SJR, Hills CD, Carey PJ. Investigation of accelerated carbonation for the stabilisation of MSW incinerator ashes and the sequestration of CO_2. Green Chem. 2004;6:428–36.
22. Huijgen WJJ. Carbon Dioxide Sequestration by Mineral Carbonation. (PhD Thesis) Energy Research Centre of the Netherlands (2007) ISBN: 90-8504-573-8 http://edepot.wur.nl/121870.
23. Jo HY, Kim JH, Lee YJ, Lee M, Choh SJ. Evaluation of factors affecting mineral carbonation of CO_2 using coal fly ash in aqueous solutions under ambient conditions. Chem Eng J. 2012;183:77–87.
24. Pan SY, Chang EE, Chiang PC. CO_2 capture by accelerated carbonation of alkaline wastes: a review on its principles and applications. Aerosol Air Qual Res. 2012;12(5):770–91.
25. Eisinas A, Doneliene J, Baltakys K, Urbutis A. Hydrothermal synthesis of calcium aluminium hydrate-based adsorbent for the removal of CO_2. J Therm Anal Calorim. 2018;131(1):537–44.
26. Wang H, Zhang J, Wang G, Wang Q, Song T. High-temperature capture of CO_2 by Li_4SiO_4 prepared with blast furnace slag and kinetic analysis. J Therm Anal Calorim. 2018;133(2):981–9.
27. Gerdemann SJ, Oconnor WK, Dahlin DC, Penner LR, Rush H. Ex Situ aqueous mineral carbonation. Environ Sci Technol. 2007;41(7):2587–93.
28. Lackner KS, Butt DP, Wendt CH. Progress on binding CO_2 in mineral substrates. Energy Convers Manag. 1997;38:259–64.
29. Rouchon L, Favergeon L, Pijolat M. Analysis of the kinetic slowing down during carbonation of CaO by CO_2. J Therm Anal Calorim. 2013;113(3):1145–55.
30. Xie HQ, Yu QB, Zhang HT, Li P. Pyrolysis kinetics study of pine cone, corn cob & peanut shell. In: Sung WP, Kao JCM, Chen R, editors. Frontiers of energy and environmental engineering. Boca Raton: CRC Press; 2012. p. 64–8.

Publisher's Note Springer Nature remains neutral with regard to jurisdictional claims in published maps and institutional affiliations.